On a better estimate of the charge collection function in CdTe solar cells: Al_2O_3 enhanced electron beam induced current measurements

Benjamin Bissig, Martina Lingg, Carlos Guerra-Nunez, Romain Carron, Fabio La Mattina, Ivo Utke, Stephan Buecheler, Ayodhya N. Tiwari

PII: S0040-6090(16)30434-5
DOI: doi: 10.1016/j.tsf.2016.08.012
Reference: TSF 35385

To appear in: *Thin Solid Films*

Received date: 26 May 2016
Revised date: 29 July 2016
Accepted date: 4 August 2016

Please cite this article as: Benjamin Bissig, Martina Lingg, Carlos Guerra-Nunez, Romain Carron, Fabio La Mattina, Ivo Utke, Stephan Buecheler, Ayodhya N. Tiwari, On a better estimate of the charge collection function in CdTe solar cells: Al_2O_3 enhanced electron beam induced current measurements, *Thin Solid Films* (2016), doi: 10.1016/j.tsf.2016.08.012

EMRS Proceedings 2016 Contribution – TITLEPAGE

On a better estimate of the charge collection function in CdTe solar cells: Al_2O_3 enhanced electron beam induced current measurements

0JKWU

Benjamin Bissig[1*], Martina Lingg[1], Carlos Guerra-Nunez[2], Romain Carron[1], Fabio La Mattina[3], Ivo Utke[2], Stephan Buecheler[1] and Ayodhya N. Tiwari[1]

[1]Laboratory for Thin Films and Photovoltaics, Empa - Swiss Federal Laboratories for Materials Science and Technology, Ueberlandstrasse 129, 8600 Duebendorf, Switzerland

[2]Laboratory for Mechanics of Materials and Nanostructures, Empa - Swiss Federal Laboratories for Materials Science and Technology, Feuerwerkerstrasse 39, 3602 Thun, Switzerland

[3]Reliability Science and Technology Laboratory, Empa - Swiss Federal Laboratories for Materials Science and Technology, Ueberlandstrasse 129, 8600 Duebendorf, Switzerland

*Corresponding author: benjamin.bissig@empa.ch, Tel +41 58 765 4305, Fax +41 58 765 1112, Benjamin Bissig, Ueberlandstrasse 129, 8600 Duebendorf, Switzerland

On a better estimate of the charge collection function in CdTe solar cells: Al_2O_3 enhanced electron beam induced current measurements

Benjamin Bissig[1], Martina Lingg[1], Carlos Guerra-Nunez[2], Romain Carron[1], Fabio La Mattina[3], Ivo Utke[2], Stephan Buecheler[1] and Ayodhya N. Tiwari[1]

[1]Laboratory for Thin Films and Photovoltaics, Empa - Swiss Federal Laboratories for Materials Science and Technology, Ueberlandstrasse 129, 8600 Duebendorf, Switzerland

[2]Laboratory for Mechanics of Materials and Nanostructures, Empa - Swiss Federal Laboratories for Materials Science and Technology, Feuerwerkerstrasse 39, 3602 Thun, Switzerland

[3]Reliability Science and Technology Laboratory, Empa - Swiss Federal Laboratories for Materials Science and Technology, Ueberlandstrasse 129, 8600 Duebendorf, Switzerland

*Corresponding author: benjamin.bissig@empa.ch, Tel +41 58 765 4305, Fax +41 58 765 1112, Benjamin Bissig, Ueberlandstrasse 129, 8600 Duebendorf, Switzerland

Abstract

The electron beam induced current technique (EBIC) was applied to substrate configuration CdTe solar cells in order to estimate the current density loss due to incomplete charge collection. In order to improve the measurement accuracy a thin Al_2O_3 layer was deposited on the device cross section by atomic layer deposition. Absorption coefficients and internal quantum efficiency (IQE) of the CdTe absorber layer and device were derived from reflection and transmission measurements. An estimate for the IQE was then calculated from EBIC measurements for devices with and without Al_2O_3 coating. The comparison of this estimate to the measured IQE shows that the Al_2O_3 enhances the accuracy of the EBIC measurements. Details of the EBIC profile and an estimate for the residual IQE i.e. current loss are discussed. Finally, a tentative explanation for the improved accuracy of the Al_2O_3 enhanced EBIC measurement is presented.

Keywords:

Electron beam induced current, alumina, passivation, CdTe, surface recombination, chalcogenide

1. Introduction

The typical current density in substrate configuration CdS/CdTe solar cells is around 24 mA cm^{-2} [1]. This indicates around 6 mA cm^{-2} current loss when compared to the theoretical maximum [2] of 30 mA cm^{-2} achievable for a bandgap of 1.5 eV under black body irradiation. For substrate configuration CdTe solar cells it was shown that this loss is dominated by reflection and parasitic absorption [1]. The loss due to incomplete charge collection was estimated to be 0.7 mA cm^{-2} derived from device external quantum efficiency (EQE) measurements and transmission/reflection measurements on the individual window layers grown on glass [1]. This approach can overestimate the collection losses in case of residual absorber transmission and it neglects differences in refractive behavior of the window layer/glass compared to the window layer/CdTe interface.

Therefore, in this contribution electron beam induced current measurements (EBIC) measurements were performed on substrate configuration CdTe devices in order to estimate collection losses by a more direct approach and additionally gain information about the junction electrostatics.

2. Experimental details:

CdTe device processing: CdTe devices were grown in substrate configuration as discussed elsewhere [3]. The typical thickness was 4.6 µm. After current-voltage measurements additional Ni (40 nm)/Al (4 µm) contacts of $3x10^{-2}$ cm^{-2} area were evaporated onto the ZnO:Al before Al_2O_3 coating to assure robust contacting during EBIC measurements. The open circuit voltage and fill factor of the device used in this study were in the range of 840 mV and 69 % respectively.

Al_2O_3 deposition by atomic layer deposition (ALD): The cross section breaking edge was defined by scribing marks outside the active area of the device with a diamond scratcher. Then the cell was cleaved between these marks and directly transferred into a home built ALD reactor. Air exposure during sample transport to the ALD system was less than 1 minute. Sample temperature during ALD was 220 °C. Trimethyl-Aluminium (TMA 97%, Aldrich) kept at room temperature and DI water kept at 40 °C were used as ALD precursors. The ALD cycles for both precursors were defined as 1 s pulsing time followed by 10 s of exposure and 30 s of purging. The average growth per cycle at 220 °C was ~1.25 Å/cycle. Here 50 cycles (~ 6nm) were deposited to assure covering growth. Note that the thermal budget during the ALD process is expected to induce Cu diffusion and accompanying changes

in absorber conductivity and lifetime [3, 4]. However, as EBIC measurements were performed more than 24 hours after ALD these effects can be considered relaxed [4].

EBIC mounting: Silver paste and Cu wires were used to contact the devices inside the scanning electron microscope (SEM) via an ohmic bridge. Before measurements the sample shunt resistances were checked (> 1 MΩ). Note that the preamplifier input resistance and the sample internal resistance form a current divider. Because of this and as collection in the space charge region (SCR) can be assumed to be very efficient (neglecting significant interface recombination) only normalized EBIC profiles will be shown.

EBIC acquisition: A Strata FEI 235 Dual Beam with beam energy at 5 keV and current at ~ 20 pA was used. High injection currents are known to lead to ambiguous interpretation of the EBIC profiles [5]. To ensure high injection effects remain negligible, we increase the injection current up to 50-fold but no significant change in the EBIC profiles was observed (not shown). Therefore we assume a low injection regime for injection currents of 20 pA, a similar value as used by Poplawsky et al. [6]. The EBIC current was gained with $1x10^7$ V/A at an input impedance of 10 kΩ (SRS SR570). Pixel dwelling times of 50 µs, field of view around 10 µm and resolution 512^2 px were chosen. Secondary electron and EBIC signal were recorded simultaneously with a GATAN system. EBIC measurements were performed within less than 24 hours after the cleaving or oxide deposition. However, no significant change in the EBIC maps was observed when repeating the measurement several weeks later.

Al_2O_3 assisted EBIC: EBIC promises simple access to the charge carrier collection function $f(\vec{x}')$ i.e. the probability for a charge carrier to be collected as device current when generated at the location $\vec{x}$ inside the device. Figure 1 displays the measurement principle. The scanning electron beam with intensity I_{INJ} and energy E_B induces a device current that is mapped in parallel with the secondary electron signal. The induced current I_{BIC} can be approximated by Equation 1,

$$I_{BIC}(\vec{x}) = \int g\left(E_B, \vec{x}, \overrightarrow{x'}\right) f(\vec{x}')\, r(\vec{x}')dV' \qquad (1)$$

where $\vec{x}$ denotes the point of injection, $g\left(E_B, \vec{x}, \overrightarrow{x'}\right)$ is the amount of carriers generated at position $\overrightarrow{x'}$ and $r(\vec{x}')$ accounts phenomenologically for surface recombination. In the vicinity of the surface, recombination is expected to be more effective ($r(\vec{x}') \rightarrow 0$) and less effective deeper in the bulk ($r(\vec{x}') \rightarrow 1$). Here we propose to actively reduce the surface recombination by deposition of Al_2O_3. We choose an injection energy of 5 keV leading to generation depths in the range of 100 nm [7].

A Shimadzu UV-3600 spectrometer equipped with an integrating sphere was used to measure transmittance and reflectance of absorbers grown on borosilicate glass (BSG) in the range from 300 nm to 1200 nm. To increase the sensitivity above the bandgap, measurements were performed on a *d* = 0.62 µm thick CdTe layer grown on BSG and treated with $CdCl_2$, similarly as for actual devices [3]. The absorption coefficients α were then estimated as discussed below and the film thickness was determined by SEM. On finished devices R was measured and the internal quantum efficiency (IQE) derived from $IQE = EQE/(1 - R)$.

The photovoltaic (PV) parameters of the solar cells were extracted from current density-voltage (J-V) characteristics under simulated standard test conditions (1000 W/m2, 25 °C, AM1.5G) measured with a Keithley 2400 source meter with four terminal sensing. The EQE curves were obtained using a monochromator and a SR830 lock-in amplifier and chopped light from a halogen lamp.

3. Results:

Figure2 a) shows secondary electron (SE) and EBIC overlays (normalized and background level set transparent) for two devices; once with Al_2O_3 (top) and once uncoated (bottom). It can be seen that the EBIC signal extends deeper and more homogeneously in the case with Al_2O_3. Figure 2b) displays corresponding EBIC line profiles as obtained from ~ 30 µm wide horizontal averaging of the EBIC signal.

Notably, the measurements were performed on unpolished cross sections. We were not able to extract meaningful correlation between EBIC signal and crystalline microstructure. It appears however that loosely attached crystallites and regions of convex surface curvature show somewhat decreased EBIC signal. Apart from surface recombination this could however also be due to different backscattering or variations in secondary electron emission yield.

The measured peak EBIC current levels were in the range of 10 nA to 15 nA for both cases. For the Al_2O_3 case an additional ~ 700 pA EBIC peak was recorded in some distance above the main junction. As can be seen in the SEM micrograph (not shown) this is the case when the beam injects into the Ni/Al top contact and notably this effect is not observed in the uncoated case. One possible origin of this signal could be related to a charging of the oxide on the metal contact and a consequent potential buildup which in turn could lead to such small device currents that are detected.

Figure 3 shows α as estimated from transmission and reflectance measurements on a thin CdTe layer treated with $CdCl_2$. The thin layer allows measurements at energies as high as 3 eV. By comparison, when conducting the same analysis on a > 4 µm thick absorber the near-complete absorption limits this range up to ~ 1.5 eV. As an estimator for α the equation

$$\alpha(\lambda) = -1/d \ln(\frac{T_{tot}+1.3\,T_{diff}}{1-R_{tot}}), \qquad (2)$$

was used, where T_{tot}/R_{tot} denote the total transmission/reflectance and T_{diff} is the measured diffuse transmission. The term $1.3\times T_{diff}$ accounts for the light trapped inside the layer assuming a Lambertian scattering at the rough air/CdTe (n ~ 3) interface. We calculated that in this case only ~ 43 % of the diffusely scattered light will leave the opposing side of the layer. Thus the real transmission that is relevant for calculation of α is estimated to be given by $T_{tot} + 1.3\times T_{diff}$. In reality the situation is more complex due to dispersion of the refractive indexes, a likely non Lambertian scattering and possible artefacts of the integrating sphere. Here we emphasize that a correction of the optical data is mandatory to obtain meaningful estimates for α and propose a simple correction scheme.

4. Discussion:

In order to estimate the current loss due to incomplete absorption the IQE was estimated according to the equation [8]

$$IQE(\lambda) = \int_0^d f(x)g(x,\lambda)dx, \quad (2)$$

where f(x) is the charge collection probability as estimated from EBIC and *g(x,λ)* is the normalized carrier generation density approximated by

$$g(x,\lambda) = -\frac{di(x,\lambda)}{dx} = \alpha(\lambda)\, e^{-\alpha(\lambda)\, x}. \quad (3)$$

Thereby, perfect free charge carrier pair generation is assumed and generation from light reflected at the back contact is neglected.

Figure 4 shows the simulated IQE in the cases with and without Al_2O_3, as well as in the case of a perfect collection defined by *f(x)* = 1. In addition, the experimental IQE calculated from EQE and reflectance of the completed cell is shown. First, it can be seen that the simulated IQE based on the measurement without Al_2O_3 significantly underestimates the experimental data in the visible range by up to 9 % at 800 nm. In the case with Al_2O_3 coating the simulation underestimates the measurement by less than 2.5% absolute over the same range. Above 820 nm the simulation overestimates the IQE in all cases. As discussed above, more accurate determination of absorption coefficients in this region is complicated by light trapping effects which lead to an apparent increase of the absorption coefficient and thus IQE.

In the hypothesis of perfect collection, a significantly more rectangular shaped IQE is predicted by the simulation. By integration of the difference between IQE of the ideal collection case and the estimator from the Al_2O_3 EBIC measurement over the AM1.5 spectrum we calculate a current loss of ~0.9 mA cm^{-2}. Due to the apparent overestimation of α discussed above, this value does however only set an upper limit for the collection loss. Furthermore, in the order i) uncoated, ii) alumina coated and iii) ideal collection the IQE cutoff shifts towards longer wavelengths. This does indicate how critically non-ideal collection can affect the extraction of the bandgap from EQE measurements.

Apparently the predictive power of the alumina enhanced EBIC with respect to IQE is superior to measurements on uncoated cross sections. In addition, the shape of the measured EBIC profiles are significantly different. For the uncoated case the near exponential decay suggests a diffusion length of ~ 1 um. The profile obtained with Al_2O_3 coating on the other hand shows a shoulder around 2 um. This feature could speculatively be ascribed to the increased collection inside the SCR, more accurately measured by EBIC in the passivated case. Note that on a similarly processed sample, the SCR width as estimated from capacitance measurements was around 2.2 µm assuming a plate capacitor model (not shown).

A tentative explanation for the mechanism of the Al_2O_3 passivation can be based on a fixed charge related model. For Cu(In,Ga)Se_2 [9], Si [10] and InGaAs [11] it was discussed that thin layer of amorphous Al_2O_3 can be an efficient electron trap leading to upward band bending. The trapping was ascribed to oxygen-rich stoichiometry of the interface near the oxide layer in combination with a deep oxygen dangling bond acceptor [11]. The band bending leads to field effect passivation of the surface and can explain the reduced carrier recombination as compared to the uncoated case. Further details on this model were shown elsewhere [12]. In case of III-V photodiodes, cross section EBIC measurements were used to study the effectivity of aqueous $(NH_4)_2S$ treatments on surface passivation [13]. This underlines that EBIC measurements in combination with passivation layers could also help to characterize and optimize passivation layers for advanced thin film solar cell concepts as recently introduced in case of Cu(In,Ga)Se_2 [14].

5. Conclusion & Outlook:

The charge collection function in CdTe solar cells in substrate configuration was measured by EBIC measurements with an Al_2O_3 passivation layer on the probed cross section. We could show that this approach allows more accurate prediction of the device IQE and derive that the residual current loss due to non-ideal collection is less than 0.9 mA cm^{-2} in this specific device. This gives complementary and direct experimental support to earlier estimation of the collection loss based on optical measurements [1]. Furthermore, a non-exponential decay of the collection function was observed, which indicates the potential use of the approach to directly access the junction electrostatics, i.e. the width of the space charge region. Tentatively, we ascribe the improved accuracy of the measurement to negative charges present in the oxide or at the CdTe/oxide interface which in turn reduce recombination at the fragmented cross section surface.

Acknowledgements:

The authors thank Till Coester and Michael Stiefel for technical support. This work was supported by the National Research Programme "Energy Turnaround" (NRP 70) of the Swiss National Science Foundation (SNSF); the Swiss National Science Foundation [grant number 200021_149453 / 1]; and the Swiss Federal Office of Energy [SI/501145-01].

References:

[1] J. Perrenoud, L. Kranz, S. Buecheler, F. Pianezzi, A.N. Tiwari, The use of aluminium doped ZnO as transparent conductive oxide for CdS/CdTe solar cells, Thin Solid Films, 519 (2011) 7444-7448.

[2] W. Shockley, H.J. Queisser, Detailed Balance Limit of Efficiency of P-N Junction Solar Cells, J. Appl. Phys., 32 (1961) 510-519.

[3] L. Kranz, C. Gretener, J. Perrenoud, R. Schmitt, F. Pianezzi, F. La Mattina, P. Blosch, E. Cheah, A. Chirila, C.M. Fella, H. Hagendorfer, T. Jager, S. Nishiwaki, A.R. Uhl, S. Buecheler, A.N. Tiwari, Doping of polycrystalline CdTe for high-efficiency solar cells on flexible metal foil, Nat. Commun., 4 (2013) 2306.

[4] J. Perrenoud, L. Kranz, C. Gretener, F. Pianezzi, S. Nishiwaki, S. Buecheler, A.N. Tiwari, A comprehensive picture of Cu doping in CdTe solar cells, J. Appl. Phys., 114 (2013) 174505.

[5] M. Nichterwitz, T. Unold, Numerical simulation of cross section electron-beam induced current in thin-film solar-cells for low and high injection conditions, J. Appl. Phys., 114 (2013) 134504.

[6] J.D. Poplawsky, N.R. Paudel, C. Li, C.M. Parish, D. Leonard, Y.F. Yan, S.J. Pennycook, Direct Imaging of Cl- and Cu-Induced Short-Circuit Efficiency Changes in CdTe Solar Cells, Adv. Energy Mater., 4 (2014) 1400454.

[7] L. Reimer, Scanning Electron Microscopy: Physics of Image Formation and Microanalysis, Springer-Verlag, second ed., Berlin Heidelberg, 1998.

[8] R. Scheer, H.-W. Schock, Chalcogenide Photovoltaics Physics, Technologies, and Thin Film Devices, first ed.,Wiley-VCH, Weinheim, 2011.

[9] W.W. Hsu, J.Y. Chen, T.H. Cheng, S.C. Lu, W.S. Ho, Y.Y. Chen, Y.J. Chien, C.W. Liu, Surface passivation of Cu(In,Ga)Se-2 using atomic layer deposited Al2O3, Appl. Phys. Lett., 100 (2012) 023508.

[10] B. Hoex, J.J.H. Gielis, M.C.M.V. de Sanden, W.M.M. Kessels, On the c-Si surface passivation mechanism by the negative-charge-dielectric Al2O3, J. Appl. Phys., 104 (2008) 113703.

[11] B. Shin, J.R. Weber, R.D. Long, P.K. Hurley, C.G. Van de Walle, P.C. McIntyre, Origin and passivation of fixed charge in atomic layer deposited aluminum oxide gate insulators on chemically treated InGaAs substrates, Appl. Phys. Lett., 96 (2010) 152908.

[12] B. Bissig, C.-N. Guerra-Nunez, R. Carron, S. Nishiwaki, F. La Mattina, F. Pianezzi, P. A. Losio, E. Avancini, P. Reinhard, S. Haass, M. Lingg, T. Feurer, I. Utke, S. Buecheler, A. N. Tiwari, Surface passivation for reliable measurement of bulk electronic properties of heterojunction devices, Small, DOI: 10.1002/smll.201601575, (2016).

[13] J.V. Li, S.L. Chuang, E. Aifer, E.M. Jackson, Surface recombination velocity reduction in type-II InAs/GaSb superlattice photodiodes due to ammonium sulfide passivation, Appl. Phys. Lett., 90 (2007) 223503.

[14] B. Vermang, V. Fjällström, J. Pettersson, P. Salomé, M. Edoff, Development of rear surface passivated Cu(In,Ga)Se2 thin film solar cells with nano-sized local rear point contacts, Sol. Energ. Mat. Sol. Cells., 117 (2013), 505-511.

List of Figures:

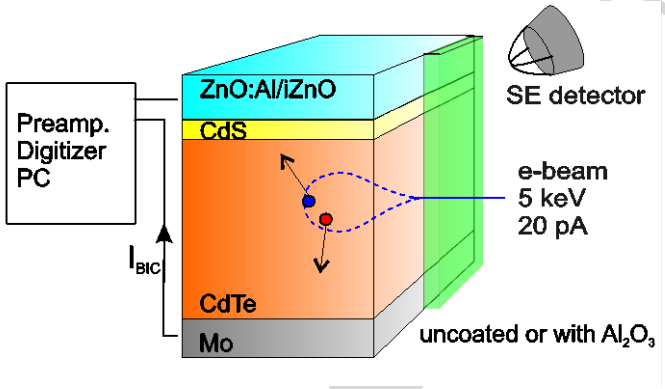

Figure 1: Experimental schematic for junction EBIC measurements: The SEM electron beam (current I_{INJ} , energy E_B) scans the cross section of the electrically connected device and the induced current I_{BIC} is mapped simultaneously to the secondary electron signal. Measurements were performed without and with a 6nm Al_2O_3 coating on the cross section.

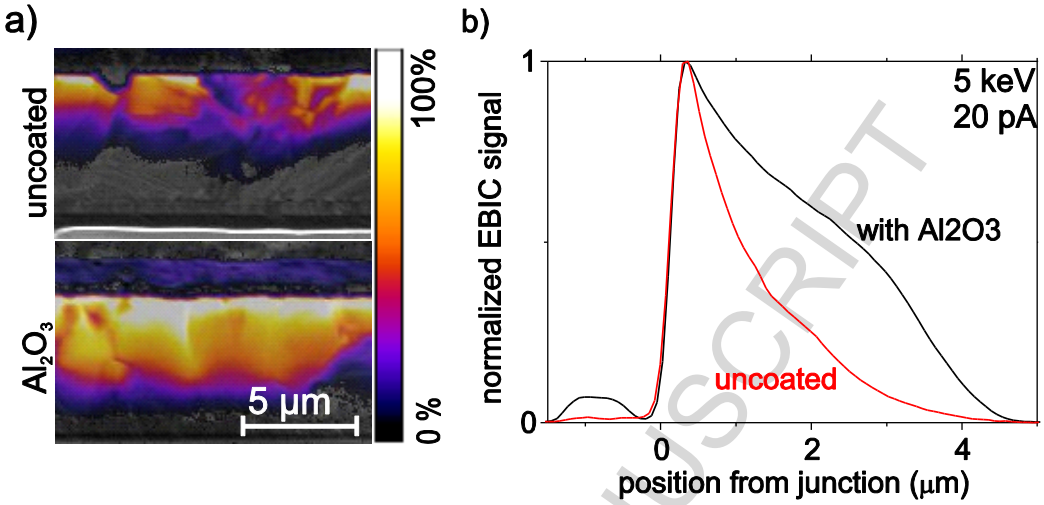

Figure 2: a) EBIC and SE overlays for CdTe devices without (top) and with (bottom) Al_2O_3 coating. The EBIC signal extends farther and more homogenously towards the back contact in case of Al_2O_3 coating. b) Normalized EBIC profiles, horizontally averaged over 30 µm are shown as solid lines for the two cases.

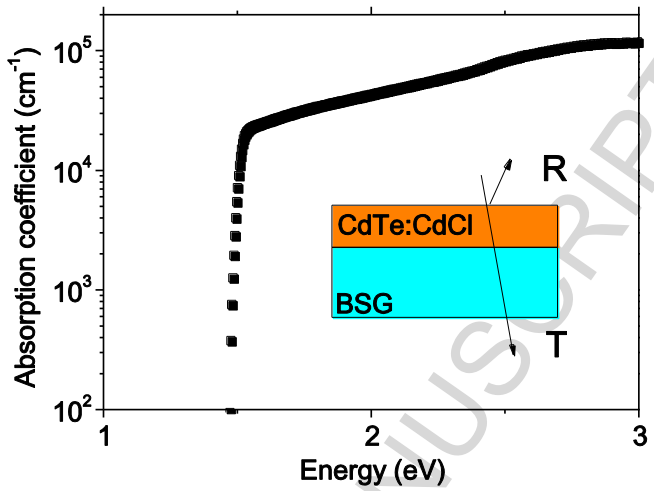

Figure 3: Absorption coefficients as estimated from transmission and reflectance measurements on 0.62 µm thick and $CdCl_2$ treated CdTe layers grown on borosilicate glass.

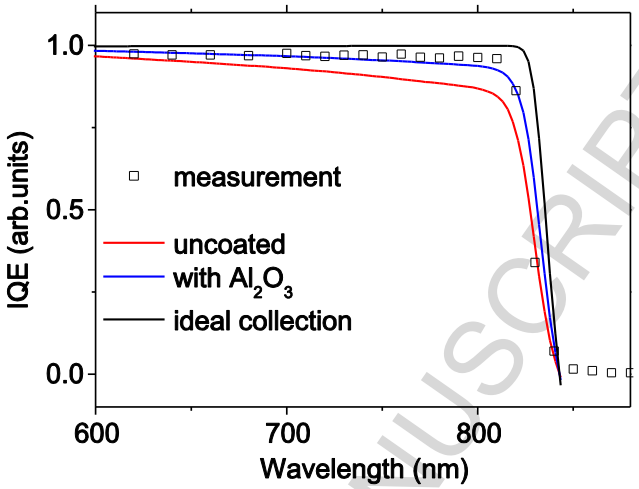

Figure 4: Comparison of measured (squares) and calculated (solid lines) IQE. Calculations are based on EBIC measurements with Al_2O_3 (blue), uncoated (red) and assuming ideal collection (black).

Highlights

- EBIC measurements were perfomed on CdTe devices
- Atomic layer deposited Al_2O_3 was deposited onto the samples before measurement
- EBIC accuracy with Al_2O_3 is found to be improved
- Current loss due to non-ideal absorption is estimated to be less than 0.5 mA cm^{-2}